Kovove Mater. 52 2014 337–344
DOI: 10.4149/km_2014_6_337

Relation between microstructural features and mechanical properties in oxygen free high conductivity copper after Equal-Channel Angular Pressing

T. Kvačkaj[1]*, A. Kováčová[1], R. Kočiško[1], J. Dutkiewicz[2], L. Lityńska-Dobrzyńska[2], J. Kansy[3]

[1]*Department of Metals Forming, Faculty of Metallurgy, Technical University in Košice, Vysokoškolská 4, 042 00 Košice, Slovak Republic*
[2]*Institute of Metallurgy and Materials Science of the Polish Academy of Sciences, W. Reymonta 25, 30 059 Kraków, Poland*
[3]*Institute of Material Science, University of Silesia, Bankowa 12, 40 007 Katowice, Poland*

Received 11 October 2013, received in revised form 10 April 2014, accepted 20 August 2014

Abstract

An oxygen free high conductivity (OFHC) copper was subjected to maximum 13 ECAP passes to achieve a sufficiently high degree of deformation. Strength properties (yield stress and ultimate tensile strength) show obvious increase up to the 4^{th} pass. In the 6^{th} ECAP pass, the yield stress and ultimate tensile strength are stabilized at a maximum of 449 MPa. Microstructure studies showed that the 1^{st} ECAP pass caused a significant increase of dislocation density. These dislocations are arranged in cells, forming dense dislocation walls at low-angle subgrains. After the 5^{th} ECAP pass, well-defined equiaxed ultrafine grains of diameter approximately 500 nm had emerged forming high-angle grain boundaries. The defect density studies carried out by positron annihilation spectroscopy method revealed an increase in a defect density (vacancies, dislocations) up to the 4^{th} pass, consequently with number of ECAP passes increasing, decrease in defects density (seen by positrons) was observed.

K e y w o r d s: dislocation, grain boundaries, equiaxed ultrafine grained microstructure, electron microscopy, Equal Channel Angular Pressing (ECAP)

1. Introduction

Refinement of material internal structure to submicrometer range has a positive impact on its final properties. An ultrafine-grained (UFG) material with an average grain size in the range of 1–0.1 μm provides advanced properties such as high strength, enhanced ductility [1, 2], suitable corrosion resistance [3]. One of the approaches to prepare the bulk UFG materials is a method of Severe Plastic Deformation (SPD) when a sample is being deformed under high strains. High Pressure Torsion (HPT) and Equal-Channel Angular Pressing (ECAP) belong to a SPD methods group and nowadays they have been successfully applied for the achievement of UFG structures [4–13]. However, a deformation mechanism as well as a material structure evolved during SPD processing show specific features which are different to conventional metal forming processes [4, 14, 15]. According to the authors [16], considering microstructure formation, severe plastic deformation methods differ from the conventional cold working techniques. During SPD processing, microstructural evolution is related to subgrain formation, evolution of the cells, types of boundaries, nucleation and growth processes as well as dislocation behaviour. Moreover, the authors [14] imply that deformation mechanism in UFG materials includes slip of perfect and partial dislocations, deformation twinning, stacking faults, grain-boundary sliding and grain rotation. The effect of lattice defects, particularly evolution of lattice dislocations and vacancies as well as their impact on specific properties of UFG materials during SPD processing is not yet understood. Such features as a change in dislocation density, formation of ultrafine grains and reduction in grain size during SPD processes can con-

*Corresponding author: tel./fax: +421-55-6024258; e-mail address: tibor.kvackaj@tuke.sk

siderably improve material mechanical properties [17, 18].

Nowadays, to recognize the deformation mechanism evolving in ultrafine-grained and nanocrystalline materials, methods as an electron microscopy and selected area diffraction patterns [19–23], positron annihilation spectroscopy [24], electron backscattered diffraction [23, 25, 26] have been used. Even, some authors have been describing a deformation mechanism in UFG materials through the study of material properties [17, 18, 27]. It is suggested that grain boundaries are to be the main sites for vacancy storage probably in the form of voids or free volume [28]. In view of these results it is therefore important to measure exactly the changes of vacancies density using positron annihilation spectroscopy in correlation with grain refinement during ECAP, which is the aim of this paper. The study of properties and microstructural features of OFHC copper subjected to different ECAP passes was performed to describe the deformation mechanism leading to UFG structures formation in a material. To study the deformation processes and microstructural evolution during ECAP, pure copper was chosen due to its FCC structure, medium stacking fault energy and its long research history considering conventional techniques such as rolling, drawing, compression [24].

The aim of the present work is to study the specific microstructural features evolving in OFHC copper subjected to ECAP processing and to contribute to the description of plastic deformation mechanism responsible for a UFG structure formation. Using methods as an electron microscopy and positron annihilation spectroscopy, evolving specific microstructural features in an OFHC copper subjected to 1–13 ECAP passes and their impact on properties were investigated. At the end, the paper also provides a discussion about plastic deformation mechanisms responsible for unexpected properties of UFG metals with focus on the contribution of this study and the mechanisms proposed by several authors, as well.

2. Experimental materials and procedures

An OFHC copper with purity above 99.99 % after zonal refining with the initial grain diameter of 40 μm was used in this study. The copper rods of cylindrical cross section (diameter 10 mm, length 100 mm) were subjected to different ECAP routes (1–13 passes) using a die with $\varphi = 90°$, $\psi = 0°$. The samples were rotated according to the route C (a sample was rotated by 180° between passes), and the experiment was carried out at the room temperature.

The structure investigations were performed using electron microscopy methods, namely Scanning Electron Microscopy (SEM) with Electron Back Scattered Diffraction (EBSD) analysis and Transmission Electron Microscopy (TEM) with Selected Area Diffraction Patterns (SADP). Samples for the electron microscopy observations were cut along an ECAP process direction and thinned using Tenupol-5 double jet electro-polisher in electrolyte 1/3 HNO_3 and 2/3 CH_3OH at subzero temperatures. The TEM and SEM analyses were performed using FEI TECNAI G2 F20 S-TWIN and JEOL JSM 7000F FEG equipments, respectively. Uniaxial static tensile tests were carried out at the room temperature by a ZWICK testing machine using samples machined along the ECAP direction. The gauge length and diameter of the tensile samples were 28 and 4 mm, respectively. The microhardness was measured by Vickers microhardness tester with pyramidal diamond indenter subject 1 kg load (HV1). The positron annihilation lifetime spectra were measured at room temperature for non-deformed sample and for 5 different degrees of deformation, i.e., for 1, 4, 5, 7 and 13 ECAP passes. A conventional fast-fast positron lifetime spectrometer of time resolution FWHM = 240 ps and the calibration constant 6.3 ps/channel was used. The positron source of activity ca. 200 kBq, covered by 20 μm Ni Kapton foil, was placed between two pieces of the investigated sample. For each sample a series of lifetime spectra was recorded. Then, the particular spectra were added up. During the adding procedure (made with a "Spectra Norm" software [29]), a correction of the spectrometer "zero drift" was carried out. This way the resultant spectra were "smooth" and of high statistics of order of 10^7 counts. The data were analysed with LT10 software [29, 30]. The apparatus parameters describing the source contribution and shape of the resolution curve were established with the help of Si, In and Sn standard samples, according to the procedure described in detail in [29].

3. Results

3.1. Mechanical properties and microhardness

The engineering stress-strain curves were drawn from the room temperature uniaxial static tensile tests and consequently, a relation between mechanical properties and number of ECAP passes was established (shown in Fig. 1). Figure 1 provides a dependence of strength and plastic properties (yield stress, ultimate tensile strength, elongation and reduction of area) after ECAP passes. According to Fig. 1, after the 4^{th} ECAP pass, the yield stress (YS) and ultimate tensile strength (UTS) show the highest increase. During the 6^{th} ECAP pass, the yield stress and ultimate tensile strength are stabilized at their maximum 425 and 449 MPa, respectively (YS is very close to UTS) from initial 285 MPa. From the 6^{th} to the 14^{th} pass, curves reach a relative equilibrium state with the tend-

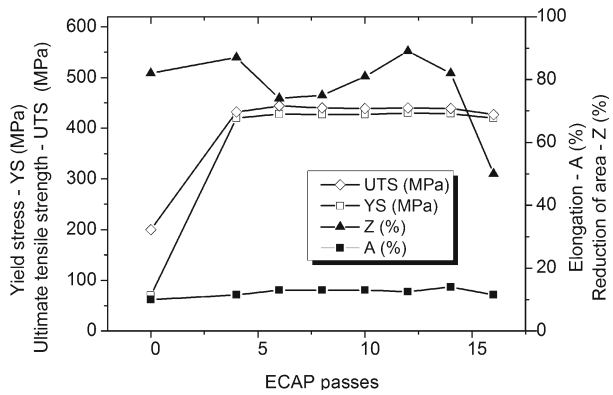

Fig. 1. Dependence of mechanical properties on ECAP passes in OFHC copper.

ency of a slow decrease. The progress of plastic properties on ECAP passes in OFHC copper is illustrated also in Fig. 1. As it can be observed, the elongation (A) is not a suitable parameter describing plastic properties because samples used for mechanical testing do not have standard geometrical parameters. Considering the reduction of area, firstly it increases (up to the 4th pass), then it decreases (up to the 6th pass). From the 6th to the 12th pass a soft increase in the reduction of area can be seen, however, afterwards a decrease was observed.

Measurements of the microhardness (HV1) on OFHC copper processed by different ECAP passes revealed almost similar progress to a strength properties progress (Fig. 1). The great increase in microhardness was seen after the 1st ECAP pass related to the increase of defects density and strain hardening [31]; microhardness attained 122 HV, as compared to the initial 47 HV (without ECAP processing). From the 2nd to 7th pass, microhardness was being raised and saturation effect was achieved in the 7th ECAP pass when microhardness was 140 HV.

3.2. Investigations of microstructural characteristics and defects

3.2.1. Electron microscopy

Figure 2 shows TEM microstructures of OFHC copper in the initial state (without ECAP processing) as well as after the 1st and 5th ECAP passes. According to Fig. 2a, dislocation density in the initial stage can be established as an intermediate (however, one cannot exclude introduction of some dislocations during the preparation process, i.e., cutting and grinding, since the initial material was very soft). No subgrains were found in the structure at this stage. Moreover, the structure contained large grains with different sizes and shapes distributed in a non-homogeneous way. After one pass (Fig. 2b), the microstructure mainly consisted of initial grains with a high density of dislocations in their interior, which were arranged to tangled dislocation (cell) and dense dislocation walls (DDWs), as it can be observed in Fig. 2b. The increase of dislocation density is in agreement with positron annihilation studies mentioned below (seen in a chapter 3.2.2) and in previous SPD studies [28, 32]. These dislocation walls usually enclose several cells and are classified as geometrically

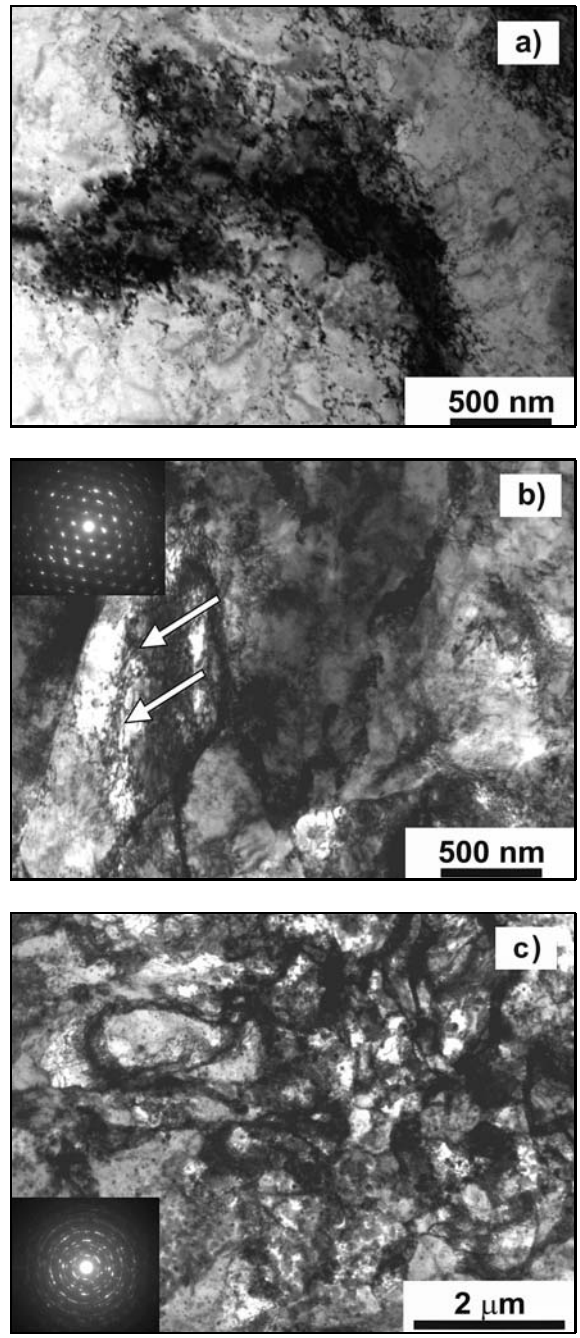

Fig. 2. TEM images of the OFHC copper: (a) without ECAP processing, (b) after the 1st ECAP pass, (c) after the 5th pass.

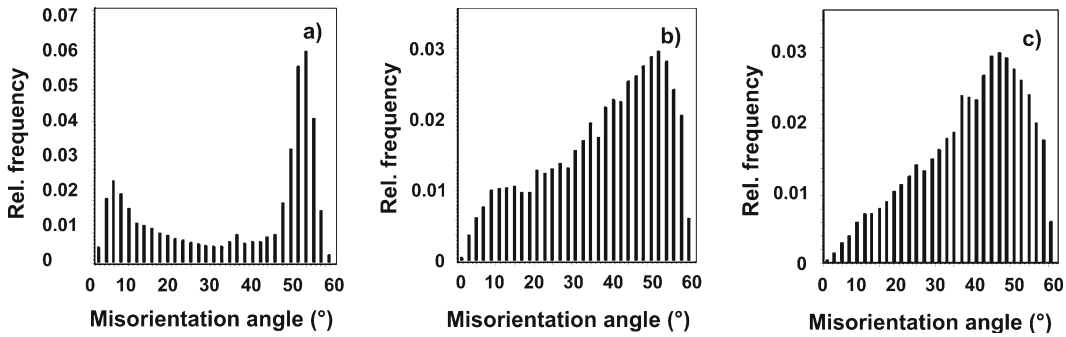

Fig. 3. Misorientation angle distribution in OFHC copper: (a) without ECAP processing, (b) after the 1st ECAP pass, (c) after the 5th pass.

necessary boundaries, since they participate in accommodation of lattice rotations in the adjoining volume [33]. Moreover, according to the authors [34], selected area diffraction observations show that these boundaries are mainly low-angle ones and are oriented along the traces of {111} planes, which indicates that they are parallel to a ⟨110⟩ shear direction. They are in a nonequilibrium state because they contain a high density of extrinsic dislocations. In some regions a tangled dislocation structure typical of heavily deformed material was observed. The investigation of material microstructure after the 5th ECAP revealed well-defined equiaxed ultrafine grains with grain size diameter of approximately 500 nm (Fig. 2c). However, the structure was still non-homogeneous and also included some large grains. Furthermore, a high degree of grain refinement as well as high subgrain misorientation was also confirmed by the SADP, where diffused reflections along Debye-Sherrer rings can be seen at much larger angles than in Fig. 2b. A decrease of grain size is connected with a decrease of vacancy concentration, and therefore it is rather suggested an annihilation of vacancy concentration than an increase of vacancy concentration at grain boundaries as suggested in [28].

Change of grain misorientation in a material subjected to ECAP processing is another specific feature. EBSD measurements provide graphical dependences shown in Fig. 3, which clearly shows that the 1st ECAP pass causes an increase of low-angle grain boundaries fraction that is similar to SADP studies carried out in [33]. Consequently, as the number of ECAP passes increase, fraction of high-angle grain boundaries is rising. Similar results in a copper processed by ECAP were confirmed by authors [24, 25]. Such differences in misorientation evolution of copper during SPD processing can have positive impact on final properties [34].

3.2.2. Positron Annihilation Spectroscopy (PAS)

According to the previous experimental work [4, 11, 15, 35, 36], severe plastic deformation introduces a vast number of defects into a material. In addition, dislocations are supposed to be responsible for formation of dislocations cell substructure that finally transforms to ultrafine grained structure.

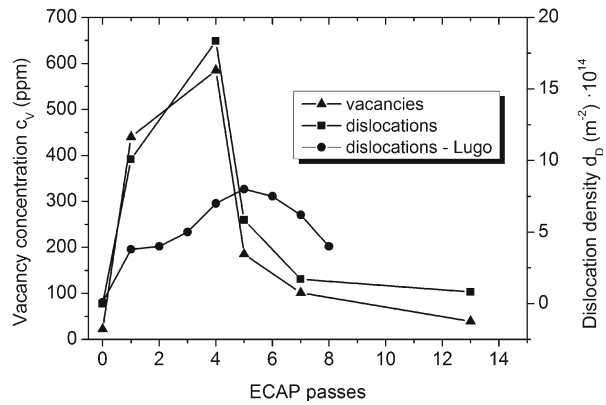

Fig. 4. PAS analysis of defects evolution on ECAP passes in OFHC copper.

Positron Annihilation Spectroscopy (PAS) is a well-developed non-destructive method with a high sensitivity to open-volume defects as vacancies, dislocations and vacancy clusters [37]. In this work, PAS was used as a tool for studying of the defects evolution. Positron Lifetime (LT) investigations on OFHC copper samples prepared by ECAP revealed the following types of defects: (a) clusters, (b) vacancies and (c) dislocations. There are indications that very high concentration of vacancies is created by severe plastic deformation also confirmed by authors [28, 32, 38]. Figure 4 provides a dependence of the defect density evolving in OFHC copper during ECAP processing. As it can be seen in Fig. 4, evolution of the defects strongly depends on the number of ECAP passes. The saturation in a defect density (vacancies and dislocations) was observed in the 4th pass, after that, with ECAP passes increasing, a decrease in defects density was observed. The author [36] also measured a dislo-

cation density in OFHC copper processed by ECAP method, the results are involved in Fig. 4. According to Lugo et al. [36], progress of dislocation density is similar to the results achieved in this work. Although, Lugo shows lower values of dislocation density and their saturation in the 5^{th} pass are probably resulting from using the different method.

According to studies of a defect density mentioned above, in a pure copper, the saturation of vacancy and dislocation density is found in the 4^{th} or 5^{th} passes, consequently, their amount is being reduced. This may result from a recovery process starting after exceeding the certain degree of deformation when after higher strains in SPD copper, a decrease in vacancy and dislocation density was seen [39]. On the other hand, the grain size is being reduced with the number of ECAP passes. The dislocations and point defects are able to reach the grain boundaries, so the defect structure becomes less homogeneous. In this way the grains of low dislocation density are surrounded by other regions with a high concentration of defects. Because of this inhomogeneity, the specific positron trapping to defects (i.e., trapping constant) decreases. In the calculations of the defect concentration (Fig. 4) the same values of positron trapping constants for samples of different numbers of ECAP were used, therefore c_V (vacancy concentration) and d_D (dislocation density) are likely underestimated and the observed decrease of c_V and d_D for large numbers of ECAP reflects the change of the defect structure rather than a decline in the defect concentrations.

4. Discussion

Generally, UFG metals offer advantageous mechanical properties what was also presented in this study (in the 3.1. section). Such progress in mechanical properties is an outcome of formation of the specific structural and mainly microstructural features in a material during SPD processing. The formation of specific structural and substructural features finally results in mechanisms of plastic deformation, which are responsible for UFG formation and typically not operative in their coarse-grained counterparts. In the present time, these plastic deformation mechanisms are still not clear. A lot of models have been proposed to account for the features of structure and mechanical properties of nanostructured materials.

The authors [14] have explained that deformation mechanism in UFG materials includes a slip of perfect and partial dislocations, deformation twinning, stacking faults, grain-boundary sliding and grain rotations. These deformation mechanisms also exist in coarse-grained (CG) materials, however, their behaviour is different. According to the authors [40], microstructure formed during SPD is usually characterized by increased dislocation and vacancy density and increased volume fraction of grain boundaries leading to increased effective diffusion coefficient. Kawasaki et al. [41] found a local small-scale grain boundary sliding in low temperatures in materials processed by ECAP. However, such grain boundary sliding is attributed to occurrence of non-equilibrium grain boundaries containing high densities of extrinsic dislocations. These extrinsic dislocations are being moved along the grain boundaries and consequently cause localized sliding, and this provides an important difference in flow characteristic between conventional metals and UFG metals prepared by SPD processing [41]. Moreover, some authors [42] have proposed "Coble creep" as a mechanism responsible for suitable correlation between strength and ductility in UFG materials, however, for having very small grains (less than 100 nm).

Chang et al. found three types of boundaries in ECAPed pure aluminium, namely polygonized dislocation wall, partially transformed boundary and grain boundary. They have proposed that during ECAP processing, polygonized dislocation walls transform firstly into partially transformed boundaries, and then into mostly high-angle grain boundaries through dissociation of lattice dislocations [43].

Evolution of microstructure in ECAPed copper is being expected from lamellar boundaries oriented parallel to the $\langle 110 \rangle$ shear direction microstructure to an equiaxed grain structure without indication of previous shear planes as was mentioned by Torre et al. [44]. They imply that cell structure is being emerged during the first pass and consequently with the increase of passes, the size of cells is stable, however, the increase of misorientation angle and the fraction of equilibrium subgrain/grain boundaries and the decrease of the width of cell walls are being carried out. Afterwards, the boundary volume fraction, and hence the total dislocation density, decrease as the number of passes increases. After the four passes, the dynamic recovery is proposed as a mechanism leading to the annihilation of dislocations, which lower the total dislocation density. This explains the restoration of the work hardening ability and consequently the increase in plastic elongation with number of passes [44].

All of specific structural and substructural features mentioned above as changes in the dislocations density, formation of ultrafine grains and the reduction in grain size during ECAP finally improve the mechanical properties [45]. On the other hand, Ferrasse et al. [18] explained that the intensive shear provides dynamic recrystallization by subgrain rotation in Cu during ECAP processing at the room temperature what has positive impact on properties. The authors [17] have explained that in the first two ECAP passes, the strain hardening characterized by dislocation motion and interaction primarily contributes

to the high strength, at the same time, grains are fragmented and subgrains are formed. As the strain increases, the generation and annihilation of dislocations gradually tends to reach a dynamic equilibrium through dynamic recovery. After four passes, grain size also cannot be obviously refined, therefore the tensile strength tends to reach saturation. Room temperature dynamic recovery is common in nanocrystalline samples. According to the authors [46], a competition between the generation of dislocations during plastic deformation and the annihilation during recovery determines the steady state dislocation density. Nevertheless, it is still questionable whether dislocations during deformation are thought to be generated from grain boundaries which also act like sinks. However, it is possible that those dislocations are still carriers of plastic deformation. As can be expected, the role of dislocations in the deformation process is difficult to determine because of their arising and disappearing in the large volume fraction of grain boundaries, and in the future, a careful investigation is needed.

According to [47], strength of the nanostructured alloys can rise either from the presence of a high density of dislocations in the grain/subgrain interior or from dislocation boundaries. This type of strengthening is typical for SPD processed pure Al or Al alloys with microstructure containing high dislocation density and high volume fraction of LAGBs, which can be fabricated via ECAP at room temperature for one to two passes [48–53]. Substructures formed through processing at low temperatures are usually referred to as cells. The misorientation of these cells is low ($\sim 1°$) and ill-defined cell walls include the tangled dislocations. Deformation at elevated temperatures results in formation of subgrained microstructures with narrow, well-defined boundaries with higher misorientation. From Hall-Petch equation, the exponent m can change from 1 to 0, 5 if the alloy undergoes the recovery process resulting in transformation of cell structures to subgrain structure [54].

According to the investigations mentioned above as well as previous experimental work [11, 15], mechanism responsible for UFG structures formation in an OFHC copper processed by ECAP is carried out through the presence of cells (subgrains) in initial grains, which are bounded with dislocations' walls having boundaries with low angle misorientations in the beginning passes. Consequently, in the following passes, transformation of the subgrain boundaries with high density of dislocations in mainly high angle grain boundaries leads to well-defined ultrafine grains formation, which was also confirmed by author [34]. Moreover, Valiev et al. [34] have described the transformation of a cellular structure to a granular one through a partial annihilation of dislocations with different signs at the cell (subgrain) boundaries at the specific time when the dislocation density in the cell walls achieved a critical value [34, 55]. Finally, excess dislocations of single sign lead to an increase of misorientation with following transformation to a granular structure.

The increase of vacancy concentration with increasing of shear deformation after ECAP passes was observed also by Schafler et al. [28, 38] up to the 5^{th} pass and no drop of vacancy or dislocation density was observed, contrary to present results. It can be partially explained by higher number of passes in the present work, however, a significant drop of vacancy density was observed already after the 5^{th} pass. At higher strains obtained by HPT [39] the drop in vacancy density, however, smaller than observed in the present paper was observed after higher strains. The difference can be explained by a different deformation mode in [39] and indirect method of measurement of vacancy concentration in [39] contrary to positron annihilation used in the present paper.

5. Conclusions

Studies of OFHC copper subjected to maximum 13 ECAP passes can be summarized as follows:

– Strength properties (yield stress and ultimate tensile strength) show obvious increase up to the 4^{th} pass. In the 6^{th} ECAP pass, the yield stress and ultimate tensile strength are stabilized at maximum 425 and 449 MPa, respectively. Microhardness revealed similar progress as the strength properties. The reduction of area shows an unexpected progress, there was found that from 6^{th} to 12^{th} pass, plasticity is rising that is out of the rules of classical mechanical hardening in cold working conditions.

– Microstructure evolution observation implies that the 1^{st} ECAP pass causes a significant increase of dislocations density. The dislocations are arranged in dislocation cells forming a dense dislocations walls (DDWs) and consequently low-angle sub grains. After the 5^{th} ECAP pass, well-defined equiaxed ultrafine grains of grain size diameter of approximately 500 nm and a large portion of a high-angle grain boundaries emerged.

– Defects density studies carried out by Positron Annihilation Spectroscopy (PAS) method revealed the increase of defects density (vacancies, dislocations) up to the 4^{th} pass, consequently with number of ECAP passes increasing, decrease in defects density was observed.

– Results obtained concerning evolution of defects density and grain size changes allow to explain the changes of mechanical properties. The increase of strength up to the 4^{th} ECAP pass is connected with the increase of dislocation and point defects density. Further stabilization of properties is connected with a decrease of grain size what is compensated by a de-

crease of defect density. The increase of plasticity is connected with an increase of grains misorientation angles allowing most probably partial grain boundary sliding contribution to the crystallographic slip.

Acknowledgement

This work was financially supported by the project VEGA 1/0359/11.

References

[1] Krasilnikov, N., Lojkowski, W., Pakiela, Z., Valiev, R.: Mater. Sci. Eng. A, *397*, 2005, p. 330. doi:10.1016/j.msea.2005.03.001

[2] Valiev, R.: Int. J. Mater. Res., *100*, 2009, p. 757. doi:10.3139/146.110095

[3] Hadzima, B., Janeček, M., Estrin, Y., Kim, H. S.: Mater. Sci. Eng. A, *462*, 2007, p. 243. doi:10.1016/j.msea.2005.11.081

[4] Valiev, R., Langdon, T.: Prog. Mater. Sci., *51*, 2006, p. 881. doi:10.1016/j.pmatsci.2006.02.003

[5] Balog, M., Simančík, F., Bajana, O., Requena, G.: Mater. Sci. Eng. A, *504*, 2009, p. 1. doi:10.1016/j.msea.2008.12.014

[6] Bidulská, J., Kočiško, R., Bidulský, R., Grande, M. A., Donič, T., Martikán, M.: Acta Metall. Slovaca, *16*, 2010, p. 4.

[7] Bidulský, R., Bidulská, J., Grande, M. A.: High Temp. Mater. Process., *28*, 2009, p. 337.

[8] Kočiško, R., Kvačkaj, T., Bidulská, J., Molnárová, M.: Acta Metall. Slovaca, *15*, 2009, p. 228.

[9] Kováčová, A., Kvačkaj, T., Kvačkaj, M., Pokorný, I., Bidulská, J., Tiža, J., Martikán, M.: Acta Metall. Slovaca, *16*, 2010, p. 91.

[10] Kvačkaj, T., Zemko, M., Kočiško, R., Kuskulič, T., Pokorný, I., Besterci, M., Sülleiová, K., Molnárová, M., Kováčová, A.: Kovove Mater., *45*, 2007, p. 249.

[11] Kvačkaj, T., Kováčová, A., Kvačkaj, M., Pokorný, I., Kočiško, R., Donič, T.: Mater. Lett., *64*, 2010, p. 2344. doi:10.1016/j.matlet.2010.07.047

[12] Yang, Z., Welzel, U.: Mater. Lett., *59*, 2005, p. 3406. doi:10.1016/j.matlet.2005.05.077

[13] Bernáthová, I., Milkovič, O.: Chem. Listy, *105*, 2011, p. 645.

[14] Zhu, Y. T., Han, B. Q., Lavernia, E. J.: Bulk Nanostructured Materials. Weinheim, WILEY-VCH Verlag GmbH & Co. KGaA 2009.

[15] Kvačkaj, T., Kováčová, A., Kvačkaj, M., Kočiško, R., Lityńska-Dobrzyńska, L., Stoyka, V., Mihaliková, M.: Micron, *43*, 2012, p. 720. doi:10.1016/j.micron.2012.01.003

[16] Kibar, A. A, Tan, E., Gür, C. H.: Mater. Charact., *62*, 2011, p. 391. doi:10.1016/j.matchar.2011.01.016

[17] Wei, W., Chen, G., Wang, J., Chen, G.: Rare Metals, *25*, 2006, p. 697. doi:10.1016/S1001-0521(07)60015-1

[18] Ferrasse, S., Segal, V. M., Hartwig, K. T., Goforth, R. E.: Metall. Mater. Trans. A, *28*, 1997, p. 1047. doi:10.1007/s11661-997-0234-z

[19] Dutkiewicz, J., Kusnierz, J., Maziarz, W., Lejkowska, M., Garbacz, H., Lewandowska, M., Dobromyslav, A. V., Kurzydlowski, K. J.: Phys. Status Solidi A, *202*, 2005, p. 2309. doi:10.1002/pssa.200521235

[20] Dutkiewicz, J., Litýnska-Dobrzyńska, L., Kováčová, A., Rogal, L., Maziarz, W.: J. Microsc. (Oxford), *236*, 2009, p. 132. doi:10.1111/j.1365-2818.2009.03284.x

[21] Dutkiewicz, J., Litýnska-Dobrzyńska, L., Kováčová, A., Molnárová, M., Rogal, L., Maziarz, W.: J. Microsc. (Oxford), *237*, 2010, p. 237. doi:10.1111/j.1365-2818.2009.03230.x

[22] Kusnierz, J., Mathon, M. H., Dutkiewicz, J, Baudin, T., Jasienski, Z., Penelle, R.: Arch. Metall. Mater., *50*, 2005, p. 367.

[23] Cahng, J. Y., Yoon, J. S., Kim, G. H.: Scripta Mater., *45*, 2001, p. 347. doi:10.1016/S1359-6462(01)01040-5

[24] Janeček, M., Čížek, J., Dopita, M., Král, R., Srba, O.: Mater. Sci. Forum, *584–586*, 2008, p. 440. doi:10.4028/www.scientific.net/MSF.584-586.440

[25] Mishra, A., Richard, V., Gregori, F., Kad, B., Asaro, R. J., Meyers, M. A.: Mater. Sci. Forum, *503–504*, 2006, p. 25. doi:10.4028/www.scientific.net/MSF.503-504.25

[26] Rusz, S., Dutkiewicz, J., Faryna, M., Maziarz, W., Rogal, L., Bogucka, J., Malanik, K., Kedroň, J., Tylšar, S.: Solid State Phenomena, *186*, 2012, p. 94. doi:10.4028/www.scientific.net/SSP.186.94

[27] Habibi, A., Ketabchi, M., Eskandarzadeh, M.: J. Mater. Process. Technol., *211*, 2011, p. 1085. doi:10.1016/j.jmatprotec.2011.01.009

[28] Ungár, T, Schafler, E., Hanak, P., Bernstorff, S., Zehetbauer, M.: Mater. Sci. Eng. A, *462*, 2007, p. 398. doi:10.1016/j.msea.2006.03.156

[29] Giebel, D., Kansy, J.: Physics Procedia, *35*, 2012, p. 122. doi:10.1016/j.phpro.2012.06.022

[30] Kansy, J.: Nucl. Instrum. Meth. A, *374*, 1996, p. 235. doi:10.1016/0168-9002(96)00075-7

[31] Shaarbaf, M., Toroghinejad, M. R.: Mater. Sci. Eng. A, *473*, 2008, p. 28. doi:10.1016/j.msea.2007.03.065

[32] Zehetbauer, M., Kohout, J., Schafler, E., Sachslehner, F., Dubravina, A.: J. Alloys Compd., *378*, 2004, p. 329. doi:10.1016/j.jallcom.2004.01.039

[33] Kužeľ, R., Janeček, M., Matěj, Z., Čížek, J., Dopita, M., Srba, O.: Metall. Mater. Trans. A, *41*, 2010, p. 1174. doi:10.1007/s11661-009-9895-0

[34] Valiev, R. Z., Islamgaliev, R. K., Alexandrov, I. V.: Prog. Mater. Sci., *45*, 2000, p. 103. doi:10.1016/S0079-6425(99)00007-9

[35] Čížek, J., Janeček, M., Srba, O., Kužeľ, R., Barnovská, Z., Procházdka, I., Dobatkin, S.: Acta Mater., *59*, 2011, p. 2322. doi:10.1016/j.actamat.2010.12.028

[36] Lugo, N., Llorca, N., Sunol, J. J., Cabrera, J. M.: J. Mater. Sci., *45*, 2010, p. 2264. doi:10.1007/s10853-009-4139-7

[37] Hautojärvi, P.: Positrons in Solids. Berlin, Springer Verlag 1979. doi:10.1007/978-3-642-81316-0

[38] Schafler, E., Steiner, G., Korznikova, E., Kerber, M., Zehetbauer, M. J.: Mater. Sci. Eng. A, *410–411*, 2005, p. 169. doi:10.1016/j.msea.2005.08.070

[39] Setman, D., Schafler, E., Korznikova, E., Zehetbauer, M. J.: Mater. Sci. Eng. A, *493*, 2008, p. 116. doi:10.1016/j.msea.2007.06.093

[40] Sauvage, X., Wilde, G., Divinski, S. V., Horita, Z., Valiev, R. Z.: Mater. Sci. Eng. A, *540*, 2012, p. 1. doi:10.1016/j.msea.2012.01.080
[41] Kawasaki, M., Balasubramanian, N., Langdon, T. G.: Mater. Sci. Eng. A, *528*, 2011, p. 6624. doi:10.1016/j.msea.2011.05.005
[42] Masumura, R. A., Hazzledine, P. M., Pande, C. S.: Acta Mater., *46*, 1998, p. 4527. doi:10.1016/S1359-6454(98)00150-5
[43] Chang, C. P., Sun, P. L., Kao, P. W.: Acta Mater., *48*, 2000, p. 3377. doi:10.1016/S1359-6454(00)00138-5
[44] Torre, F. D., Lapovok, R., Sandlin, J., Thomson, P. F., Davies, C. H. J., Pereloma, E. V.: Acta Mater., *52*, 2004, p. 4819. doi:10.1016/j.actamat.2004.06.040
[45] Kibar, A. A., Tan, E., Gür, C. H.: Mater. Charact., *62*, 2011, p. 391. doi:10.1016/j.matchar.2011.01.016
[46] Meyers, M. A., Mishra, A., Benson, D. J.: Prog. Mater. Sci., *51*, 2006, p. 427. doi:10.1016/j.pmatsci.2005.08.003
[47] Sabirov, I., Murashkin, M. Yu., Valiev, R. Z.: Mater. Sci. Eng. A, *560*, 2013, p. 1. doi:10.1016/j.msea.2012.09.020
[48] Chinh, N. Q., Gubicza, J., Czeppe, T., Lendvai, J., Xu, C., Valiev, R. Z., Langdon, T. G.: Mater. Sci. Eng. A, *516*, 2009, p. 248. doi:10.1016/j.msea.2009.03.049
[49] Duan, Z. C., Chinh, N. Q., Xu, C., Langdon, T. G.: Metall. Mater. Trans. A, *41*, 2010, p. 802. doi:10.1007/s11661-009-0020-1
[50] Venkateswarlu, K., Ghosh, M., Ray, A. K., Xu, C., Langdon, T. G.: Mater. Sci. Eng. A, *485*, 2008, p. 476. doi:10.1016/j.msea.2007.08.007
[51] Cepeda-Jimenez, C. M., Garcia-Infanta, J. M., Ruano, O. A., Carreno, F.: J. Alloys Compd., *509*, 2011, p. 8649. doi:10.1016/j.jallcom.2011.06.070
[52] El-Danaf, E. A.: Mater. Des., *32*, 2011, p. 3838. doi:10.1016/j.matdes.2011.03.006
[53] Kim, W. J., Wang, J. Y.: Mater. Sci. Eng. A, *464*, 2007, p. 23. doi:10.1016/j.msea.2007.03.074
[54] Polmear, I. J.: Light Alloys: From Traditional Alloys to Nanocrystals. 4th ed. Oxford, Elsevier 2006.
[55] Zhu, Y. T., Langdon, T. G.: Mater. Sci. Eng. A, *409*, 2005, p. 234. doi:10.1016/j.msea.2005.05.111